

# Federated Foundation Model for Cardiac CT Imaging

Malte Tölle<sup>1,2,3</sup>, Philipp Garthe<sup>4</sup>, Clemens Scherer<sup>1,5</sup>, Jan Moritz Seliger<sup>1,6</sup>, Andreas Leha<sup>1,7</sup>, Nina Krüger<sup>1,8,9,10</sup>, Stefan Simm<sup>1,11</sup>, Simon Martin<sup>1,12</sup>, Sebastian Eble<sup>2</sup>, Halvar Kelm<sup>2</sup>, Moritz Bednorz<sup>2</sup>, Florian André<sup>1,2,3</sup>, Peter Bannas<sup>1,6</sup>, Gerhard Diller<sup>4</sup>, Norbert Frey<sup>1,2,3</sup>, Stefan Groß<sup>1,11</sup>, Anja Hennemuth<sup>1,6,8,9,10</sup>, Lars Kaderali<sup>1,11</sup>, Alexander Meyer<sup>1,8</sup>, Eike Nagel<sup>1,12</sup>, Stefan Orwat<sup>4</sup>, Moritz Seiffert<sup>13</sup>, Tim Friede<sup>1,7</sup>, Tim Seidler<sup>1,14,15</sup>, and Sandy Engelhardt<sup>1,2,3</sup>

<sup>1</sup> DZHK (German Centre for Cardiovascular Research), all partner sites

<sup>2</sup> Department of Cardiology, Angiology and Pneumology, Heidelberg University Hospital, Heidelberg, Germany

<sup>3</sup> Informatics for Life Institute, Heidelberg, Germany

<sup>4</sup> Clinic for Cardiology III, University Hospital Münster, Münster, Germany

<sup>5</sup> Department of Medicine I, LMU University Hospital, LMU Munich, Munich, Germany

<sup>6</sup> Department of Diagnostic and Interventional Radiology and Nuclear Medicine, University Medical Center Hamburg-Eppendorf, Hamburg, Germany

<sup>7</sup> Department of Medical Statistics, University Medical Center Göttingen, Göttingen, Germany

<sup>8</sup> Deutsches Herzzentrum der Charité (DHZC), Institute of Computer-assisted Cardiovascular Medicine, Berlin, Germany

<sup>9</sup> Charité – Universitätsmedizin Berlin, corporate member of Freie Universität Berlin and Humboldt-Universität zu Berlin, Berlin, Germany

<sup>10</sup> Fraunhofer Institute for Digital Medicine MEVIS, Bremen, Germany

<sup>11</sup> Institute of Bioinformatics, University Medicine Greifswald, Greifswald, Germany

<sup>12</sup> Institute for Experimental and Translational Cardiovascular Imaging, Goethe University, Frankfurt am Main, Germany

<sup>13</sup> Department of Cardiology, University Heart and Vascular Center Hamburg, University Medical Center Hamburg-Eppendorf, Hamburg, Germany

<sup>14</sup> Department of Cardiology, University Medicine Göttingen, Göttingen, Germany

<sup>15</sup> Department of Cardiology, Campus Kerckhoff of the Justus-Liebig-Universität at Gießen, Kerckhoff-Clinic, Gießen, Germany

malte.toelle@med.uni-heidelberg.de

**Abstract.** Federated learning (FL) is a renowned technique for utilizing decentralized data while preserving privacy. However, real-world applications often involve inherent challenges such as partially labeled datasets, where not all clients possess expert annotations of all labels of interest, leaving large portions of unlabeled data unused. In this study, we conduct the largest federated cardiac CT imaging analysis to date, focusing on partially labeled datasets ( $n = 8,124$ ) of Transcatheter Aortic Valve Implantation (TAVI) patients over eight hospital clients. Transformer architectures, which are the major building blocks of current foundation models, have shown superior performance when trained on larger cohorts than traditional CNNs. However, when trained on small task-specific labeled sample sizes, it is currently not feasible to exploit their underlying attention mechanism for improved performance. Therefore, we developed a two-stage semi-supervised learning strategy that distills knowledge from several task-specific CNNs (landmark detection and segmentation of calcification) into a single transformer model by utilizing large amounts of unlabeled data typically residing unused in hospitals to mitigate these issues. This method not only improves the predictive accuracy and generalizability of transformer-based architectures but also facilitates the simultaneous learning of all partial labels within a single transformer model across the federation. Additionally, we show that our transformer-based model extracts more meaningful features for further downstream tasks than the UNet-based one by only training the last layer to also solve segmentation of coronary arteries. We make the code and weights of the final model openly available, which can serve as a foundation model for further research in cardiac CT imaging.

## 1 Introduction

The manual annotation of medical images is a laborious task that requires expert knowledge [41,38]. Often, physicians can only label a limited amount of data for deep learning model training. They typically focus on labeling data relevant to their specific research needs, leaving a significant portion of data unlabeled and thus unused for training. As a result, small, highly specialized subsets of large, mostly unlabeled datasets are common in local clinics. This presents two opportunities for improvement. First, the training data can be enlarged by leveraging all labeled subsets across clinics, while accounting for the different structures annotated in each. Second, by leveraging labeled and unlabeled datasets in a pooled training synergy effects can be realized, if over all participating hospitals every label of interest is present in at least one location. Additionally, the diversity of training data from various institutions can expand the overall training distribution (Fig. 1).

Privacy laws hinder the widespread collection of such heterogeneous large scale datasets stored at a single location<sup>1</sup>. Federated Learning (FL) is one paradigm that circumvents privacy concerns by reverting the paradigm of central data storage [40,18,17,42]. In FL, the model is distributed to all data holding institutions, where training is performed locally before the model is sent back to a central server. On this server the trained model weights from all participating clients are averaged before another round of training is initialized (see Fig. 1). Unfortunately, the quality and consistency of labels across different clients can vary, impacting the model’s performance. Without inspection from the data scientist label quality and consistency must be ensured in FL, which often poses a big challenge that impedes the predictive performance of federated trained models on real world data [18].

In situations where each institution has a different subset of the total training labels, the clients are termed partially labeled. Training on such clients requires complex algorithms for handling the loss computation on clients, where labels are not present. Partially labeled data can further result in a skewed distribution of labels across clients. Some labels might be overrepresented in the overall dataset, while others are underrepresented. This can lead to biased models that perform well on some labels of data but poorly on others. Training a single model to effectively address all tasks across these clients is challenging due to the uneven distribution of annotations.

The largest FL study on 3D medical images to date ( $n = 6,314$ ) was performed by [35], who trained an automatic tumor boundary detector for the rare disease of glioblastoma in a federated manner. They reported improvement over a publicly trained model especially on rare cases that are not represented in rather small public datasets. Other works include the prediction of future oxygen requirement of COVID 19 patients and the histological response to breast cancer [9,49]. The largest federated learning study in cardiovascular imaging is conducted by Linardos et al. [24]. They use subsets of the publicly available magnetic resonance imaging (MRI) datasets from the Multi-Centre, Multi-Vendor, and Multi-Disease Cardiac Image Segmentation Challenge (M&Ms) and Automated Cardiac Diagnosis Challenge (ACDC) with 180 patients in total [6,5]. In all the aforementioned studies, it is assumed that all clients possess all labels available in the federation. However, the scenario of partially labeled clients has not been considered.

All approaches report an increase in generalizability for the federated trained model compared to the individual trained one. However, in all reported studies on real world data the labels were consistently distributed across all participating clients in the federation. To the best of our knowledge there exists no comparable study with federated learning on real world data with a similar amount of data on partially labeled clients. Additionally, unlabeled data is usually discarded and not used to further increase model performance. Compared to the segmentation of tumors on MR brain scans [35] our considered use case has a much larger variability in the used data.

<sup>1</sup> Health Insurance Portability and Accountability Act (HIPAA): <https://www.cdc.gov/phlp/publications/topic/hipaa.html>, General Data Protection Regulation (GDPR): <https://gdpr.eu/>

When solving imaging tasks a convolutional UNet is most often the method of choice [35,20,15,55]. Due to the inductive bias of the convolutional operations they tend to generalize better with smaller amounts of data than transformer based architectures [29]. However, recent literature on foundation models has shown promising performance of transformers when only trained on large enough dataset sizes [33,51,25]. Transformers have the advantage of a larger receptive field due to their inbuilt attention mechanism. Not exhibiting an inductive bias also becomes an advantage if only enough data samples are used. To improve the performance of both model architectures knowledge distillation (KD) can be used. In KD, usually a student network is trained to mimic output of a teacher network [14].

Diseases of the cardiovascular system amount for up to a third of deaths in developed countries<sup>2</sup>. A common valve pathology is described by aortic valve stenosis, which is a condition where the aortic valve becomes narrowed, leading to reduced blood flow from the heart to the rest of the body. A Transcatheter Aortic Valve Implantation (TAVI) is primarily performed catheter-based to replace the present valve with an artificial one. Due to its less invasive nature it has become the gold standard for treating severe aortic stenosis in patients who are considered high risk or inoperable for surgical aortic valve replacement [22,11]. However, patients receiving a TAVI are more prone to be dependent on a pacemaker post implantation due to the prosthesis applying pressure to the stimulation conduction system of the heart [43]. Known influencing parameters are the aortic valve geometry, the per-cusp calcification, and the distance of the annulus plane to the membranous septum [28,32]. The three hinge points determine the location of the aortic annulus plane, which is the location of the smallest diameter of the aortic root and thus determines the size of the prosthesis, while the coronary ostia determine the possible length. A measurement not yet taken in clinical practice is the location of the smallest part of the membranous septum and its distance from the annulus plane [16]. Multiple works exist that perform localization of aortic root and hinge points as well as coronary ostia [21,3,2]. However, all methods were trained on single site data and no method is able to quantify all aspects from the CT, which might be attributed to missing labels for some subtasks at the specific locations. Thus, the presented approaches might not generalize well outside of their training datasets. No method exists so far that combines quantification of aortic landmarks with the detection of the membranous septum and the quantification of calcification in the area of the aortic root, which are both important predictors for selecting the right prosthesis and determine the outcome after TAVI.

Within the German Center for Cardiovascular Diseases (DZHK) we have set up a federated learning infrastructure connecting eight cardiology and radiology departments of university clinics in Germany. Each institution provides the pre-TAVI computed tomography (CT) scans as well as their individual present labels that help in choosing the right prosthesis (hinge points, coronary ostia, membranous septum, and per-cusp calcification). All CT scans used in the federated training are routinely acquired in clinical practice. One caveat of dealing with real world clinical data is the heterogeneity of available labels, which is especially prominent in our use case. While the annotated hinge points and coronary ostia are labeled across all participating locations, the membranous septum as well as the calcification are only labeled at a few not completely overlapping institutions. This work shows the following contributions.

- **Study size and label scarcity:** We present the largest up to date study in cardiac computed tomography imaging from real world patient data spanning eight hospitals in Germany ( $n = 8, 124$ ). In our study, labels are scarce, meaning not all locations are in the possession of all label categories and further only a small fraction of data samples are labeled at the respective locations.
- **Federated point detection and segmentation:** We train a model for each custom task (hinge points and coronary ostia points, points of membranous septum, and segmentation of calcification) in a federated manner [15]. Due to their inductive bias convolutional neural networks can generalize better with small amounts of training samples. For guidance we feed the segmented heart as a condition such

---

<sup>2</sup> [https://www.who.int/news-room/fact-sheets/detail/cardiovascular-diseases-\(cvds\)](https://www.who.int/news-room/fact-sheets/detail/cardiovascular-diseases-(cvds))

that the models can learn the anatomical relations between heart and the corresponding structures. We show the superiority of the federated approach for each subtask.

- **Transfer into one model:** We are the first to employ federated knowledge distillation to fuse the knowledge of the per-task models into a different architecture than the teacher, a transformer network when small amounts of manual annotations are available. The two-stage approach increases the amount of training data mitigating the performance difference between transformer and convolutional UNet by semi-supervised learning.
- **Downstream task:** We show better generalizability of our trained transformer model compared to the convolutional based one on the downstream task of segmenting the coronary arteries by only finetuning the last layer. We attribute this to the learning of global context of the transformer model given sufficient data.
- **Inter-observer variability:** To quantify the influence of the inter-observer variability of the manual annotation on the final predictive performance every annotator in the clinics labeled samples of a public dataset [61]. The inter-observer variability across locations serves as a lower-bound for the performance of the model. The labels of this cohort will be made publicly available.
- **Privacy-Preserving Label Quality Visualization:** Due to its privacy by design structure FL does not enable the inspection of label quality at the participating sites. To verify consistency we compare the relative location of landmarks across locations, which does not disclose patient information but allows for qualitative privacy-preserving outlier detection in label quality.
- **Open source code and model weights:** The code will be made publicly available. Further, we release the model weights of the final transformer model, which can be used as a foundation model in cardiac CT imaging for future studies.

## 2 Results

For each local dataset 20% of the data was set apart to serve as an independent testset on which to evaluate the final models. These splits were preserved during the training of all model architectures per subtask as well as for the distilled model version. We always selected at least one location as test location for each task. For the hinge points we chose locations 6 and 7 for testing, for membranous septum we chose location 7, and for calcification we again chose location 6.

### (Semi-supervised) Federated Knowledge Distillation from Partially labeled Clients

The large subset of unlabeled medical data usually remains unused when training deep learning models. On the other hand the most advanced deep learning architectures based on the transformer architecture can only develop their full potential when trained on large scale datasets. We opt for combining both worlds by first training a conventional UNet on the labeled subsets of all the data. By employing the federated approach for all models we were able to include heterogeneous data from multiple locations and thus widen the training distribution for each submodel. Last, we predicted on the large datasets that were unlabeled. Subsequently, we trained a transformer architecture (SWIN-UNETR) [12] to mimic the output from the UNets on the large datasets. We used the federated trained UNets from all three subtasks. Thus, we condense the knowledge for all three tasks from three models into one with semi-supervised federated KD. Due to the mutual exclusiveness of the labels, the model gained one head for each subtask while using the same backbone. With this design, the network has the freedom to learn features that are task-agnostic in their backbone, e.g. features for segmenting the aortic root and for localizing the three aortic valve hinge points are likely to be rather similar. After KD, each head is fine-tuned on the expert-annotated datasets across the consortium, while leaving the weights of the backbone feature extractor fixed.

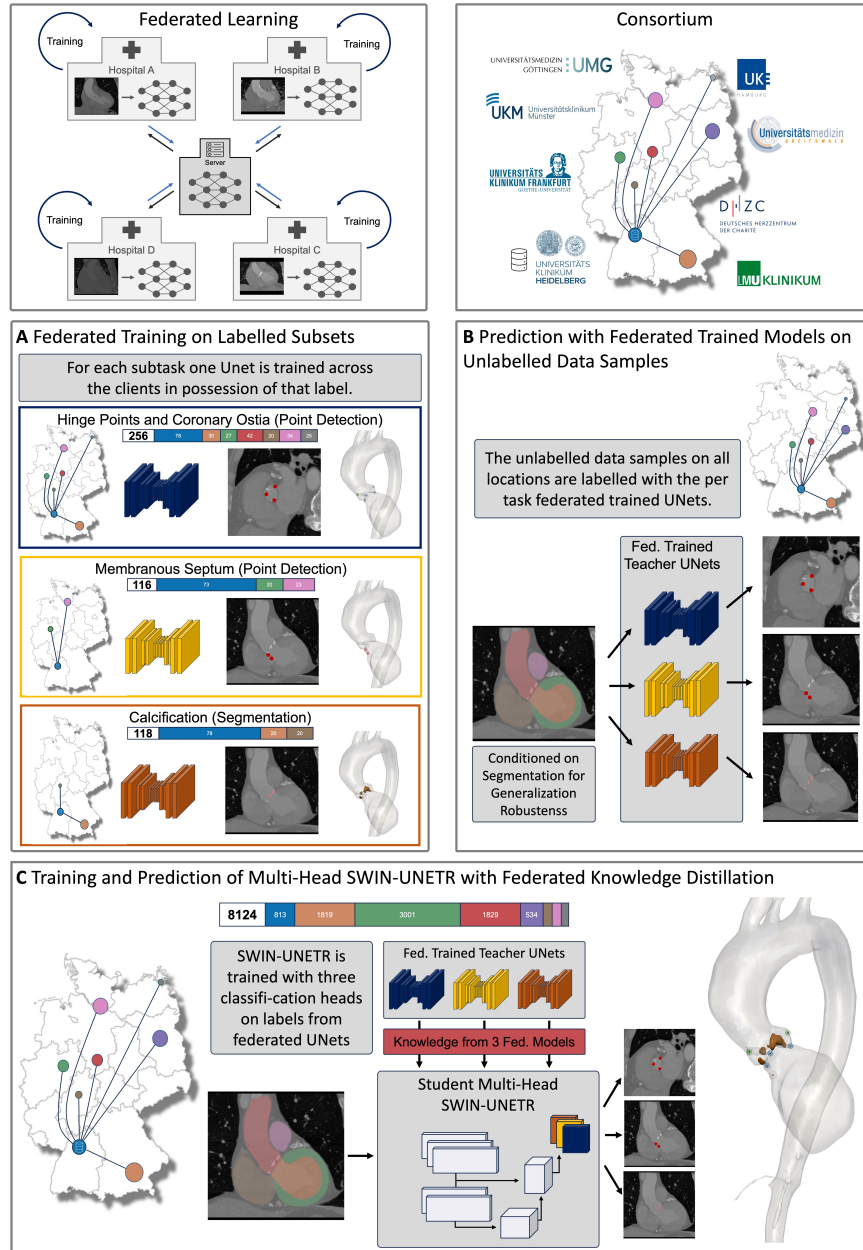


Fig. 1: Overview of federated consortium and federated knowledge distillation (KD) training pipeline. **A** Each label subset is not present at all locations. One model (UNet) is trained for each subset in a federated manner across the clients in possession of that label. **B** Subsequently, the federated trained models are used to make predictions on the unlabeled data samples. **C** The transformer based- model (SWIN-UNETR [12]) is trained from the predictions of the teacher network with three heads but the same backbone. Last, only the heads are finetuned on the human annotated data samples.

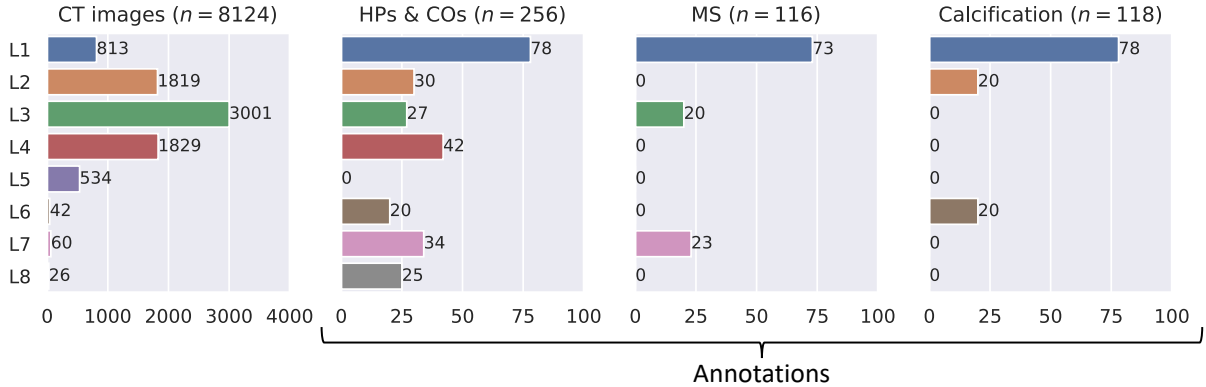


Fig. 2: Data distribution across clients. In total 8,124 CT scans are available across all eight clients. For each label the distribution is differently skewed. While the most uniform distribution is present for the hinge point training, for membranous septum and calcification the distribution is skewed. Still, the federated model that is trained over these skewed distributions exhibits better performance than the one trained on a single client. HPs & COs: Hinge Points and Coronary Ostia Points, MS: Membranous Septum.

For evaluation purposes we performed a large series of experiments comparing different architectures and local vs. federated training. For each task (point detection of hinge points, coronary ostia, membranous septum, and segmentation of calcification) three different methods are compared. First, we train a convolutional UNet and transformer-based (SWIN-UNETR) on each local dataset. Second, both models are trained in a federated fashion across the locations having labels. Third, we performed semi-supervised federated knowledge distillation on the unlabeled data of each hospital with our federated trained UNet as the teacher and a SWIN-UNETR as student, before finetuning on the labeled subsets. For federated training we always left at least one location out for training for having an independent testset in form of a completely separated client.

As can be seen in Fig. 4 models trained only on the local data shards underperform on datasets from other locations. Transformer based architectures generalize worse than convolutional UNet based ones, which we attribute to the inherent inductive bias of these architectures. The mean distance of the predicted hinge points of the local UNet approach is at  $3.09 \pm 1.71\text{mm}$  for the same location and at  $3.80 \pm 2.02\text{mm}$  for held out test locations, while the SWIN-UNETR predicts points at a mean distance of  $2.60 \pm 1.65\text{mm}$  and  $3.73 \pm 1.97\text{mm}$  respectively. Federated training improves generalization performance for both methods. However, the UNet ( $2.59 \pm 1.76\text{mm}$ ,  $3.43 \pm 1.79\text{mm}$ ) performs better than the transformer ( $3.06 \pm 1.70\text{mm}$ ,  $3.89 \pm 1.91\text{mm}$ ). While the performance of the SWIN-UNETR can be enhanced by performing semi-supervised federated knowledge distillation from the federated trained UNet on the previously unlabeled data samples at all locations the performance of the KD UNet is similar to the federated one. The predicted points lie at a mean distance of  $2.80 \pm 1.71\text{mm}$  for the training locations and  $3.36 \pm 1.83\text{mm}$  for the held out test locations for the transformer and at  $3.18 \pm 1.92\text{mm}$  and  $3.83 \pm 2.12\text{mm}$  for the UNet.

The performance for detecting the membranous septum is similar to localizing the hinge points. The UNet generalizes better with fewer data samples, but the SWIN-UNETR can be improved with semi-supervised federated knowledge distillation to even surpass the UNet on the unseen test clients. The local UNet predicts a mean distance of  $3.01 \pm 1.84\text{mm}$  on the same client and  $4.30 \pm 1.82\text{mm}$  on

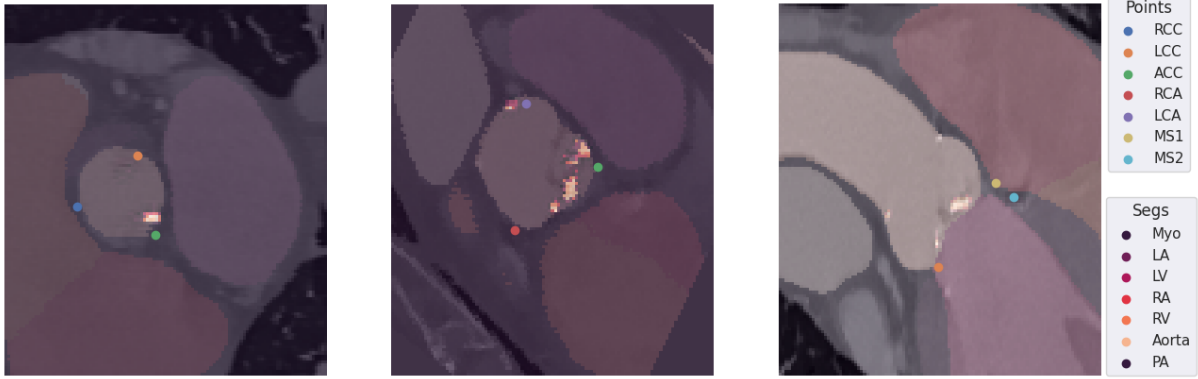


Fig. 3: Qualitative results of the predicted labels of FedKD SWIN-UNETR, which is the final distilled model. The predictions were inspected by two experienced cardiologists verifying that the points are placed within the anatomical variance present. RCC: right coronary cusp, LCC: left coronary cusp, NCC: non-coronary cusp, RCO: right coronary ostium, LCO: left coronary ostium, MS1: upper, and MS2: lower point of membranous septum, Myo: myocardium, LA: left atrium, LV: left ventricle, RA: right atrium, RV: right ventricle, PA: pulmonary artery.

others, the local transformer predicts points at  $3.96 \pm 2.19$  mm and  $4.06 \pm 2.16$  mm distance respectively. When training both models in a federated manner the SWIN-UNETR generalizes better when knowledge distillation is employed, what is seen with the lower standard deviation. The UNet’s mean distance lies at  $3.40 \pm 1.56$  mm, while the transformer’s is at  $3.29 \pm 1.45$  mm. The performance on the training clients is very similar (UNet:  $2.99 \pm 1.81$  mm, KDT:  $2.95 \pm 1.72$  mm).

Segmenting the calcification in the aortic root leads to different results than the previous tasks. The transformer performs better than the UNet especially when trained in a federated manner with a DICE score of  $68.27 \pm 20.15$  on the testsets of the training locations and  $69.15 \pm 23.23$  on the held out test location. The federated UNet only achieves a DICE score of  $49.45 \pm 20.94$  and  $39.10 \pm 21.20$  respectively. The model trained with KD is almost on par with the federated trained transformer with DICE scores of  $64.55 \pm 20.79$  and  $67.01 \pm 23.14$ . We attribute the slightly worse performance to the concurrent point detection which seems to favor partly other image features than calcification segmentation.

In conclusion, semi-supervised federated knowledge distillation enhances the predictive performance of a transformer based architecture (SWIN-UNETR) [12] to be better or on par with the Unet based counter part. Further, the tasks of locating the hinge points, coronary ostia, and membranous septum as well as segmenting the calcification of the aortic root can be solved with one model despite the distributed label classes across different classes.

### Anatomical Relations for Visual Assessment Label Quality

One crucial aspect that hinders the widespread usage of federated learning to data is the inferior label quality sometimes present at participating locations. In the centralized setting one can identify false labels from training with visual inspection. Due to its inherent privacy constraints original data such as images

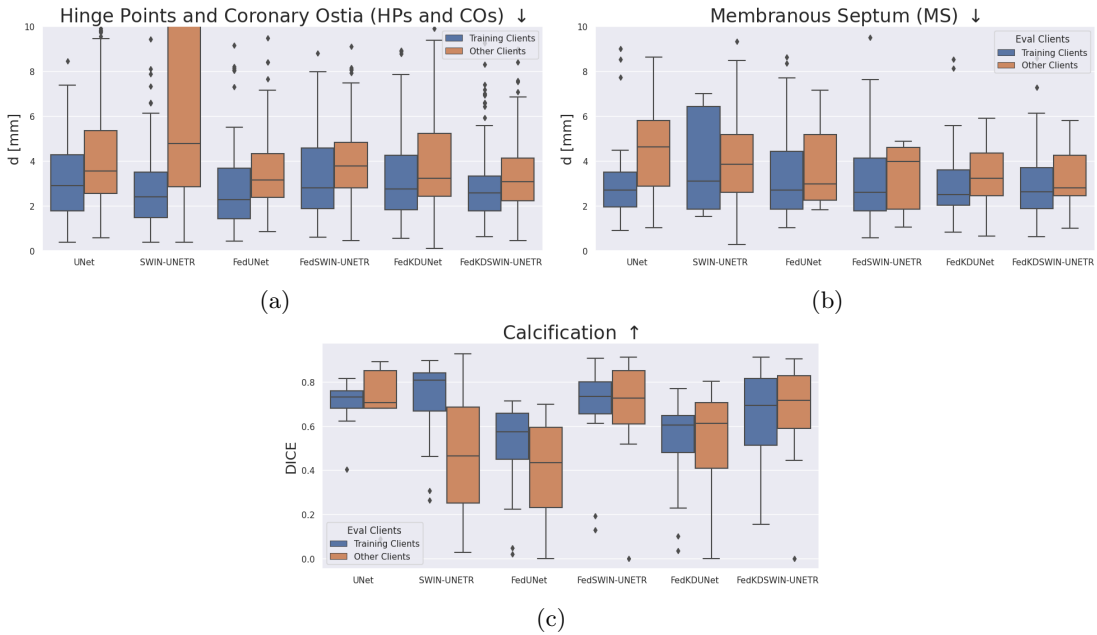


Fig. 4: Comparison of locally and federated trained UNets and transformer-based models (SWIN-UNETR). The locally trained models perform well on their client’s respective data, but do not generalize to the data from other clients. The transformer-based architecture performs worse than the UNet. The generalization performance can be enhanced with federated training, but the UNet still performs and generalizes better. After performing federated KD and subsequent finetuning the performance of the transformer-based model is on par with the UNet on detecting the hinge points, coronary ostia, and membranous septum, while outperforming it on segmenting the calcification. While the predictive performance of the SWIN-UNETR can be enhanced with more training samples due to KD to be better or on par with the UNet architecture, KD does not enhance the performance of the UNet to a similar degree. Further, the SWIN-UNETR generalizes better to other downstream tasks than the UNet based architecture.

cannot be shared and inspected, however, their annotations can be exchanged. We therefore compared the geometric relation of labels to each other across participating locations to find outliers or a systematic bias. For example, we identified a mixed up of label ids for upper and lower membranous septum point, shown in Fig. 5.

Fig. 5 shows some outliers for hinge points and membranous septum. Interestingly, the spread of labels is larger in the manual annotations, while the predictions of the network are more centered. This indicates a higher inter-observer variability, which we separately assessed in the following section. Furthermore, no confusion of point ids occurred in the predicted landmarks.

### Evaluation of Inter-Observer Variability on Public Dataset

To quantify the inter-observer variability of the manual generated ground truth to our model, we evaluated the performance of our final model on the public ImageCAS dataset [61] against each annotator from the participating locations, which has labeled 20 samples. The mean distance from the mean over all



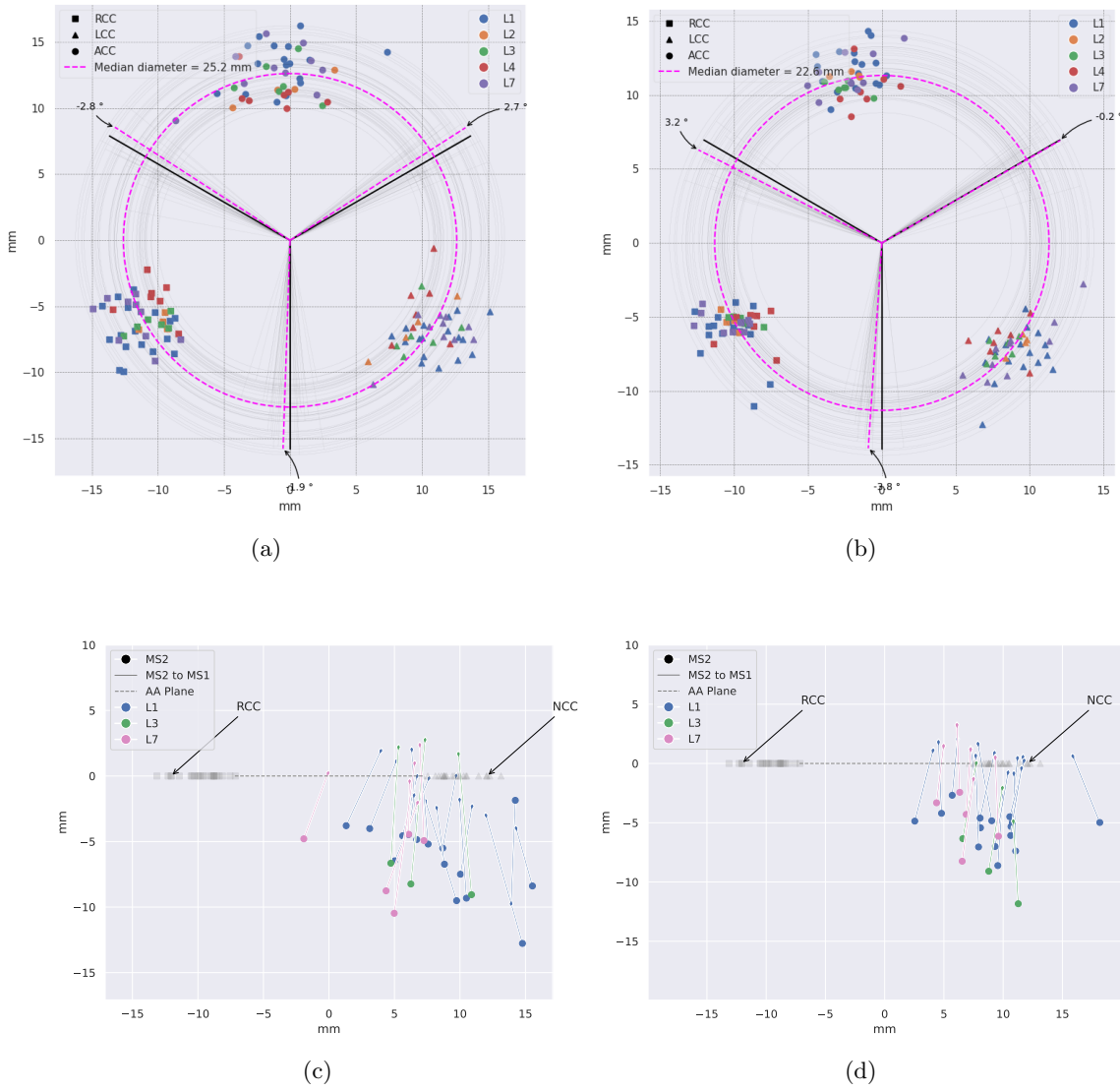


Fig. 5: Privacy-preserving inspection of labels. The overall distribution of landmarks should be similar across locations, because the geometrical relations between the points is relatively homogeneous. a) human annotated and b) model predicted hinge points, c) human annotated and d) model predicted membranous septum landmarks. In a) and b) the AA plane is defined from the three hinge points, the center point is registered, and the rotational angle is minimized to the distance from an optimal orientation of  $120^\circ$  between the three points. In c) and d) the RCC and NCC hinge points are registered and the location of the two points representing the membranous septum in relation to the two points is visualized. Thus, the overall quality of labels without disclosing any image information can be inspected. In c) MS1 and MS2 are confused (arrow points down). The spread is larger for the human annotated labels, which we attribute to slightly different annotation habits. RCC: right coronary cusp, LCC: left coronary cusp, NCC: non-coronary cusp, MS1: upper point of membranous septum, MS2: lower point of membranous septum.

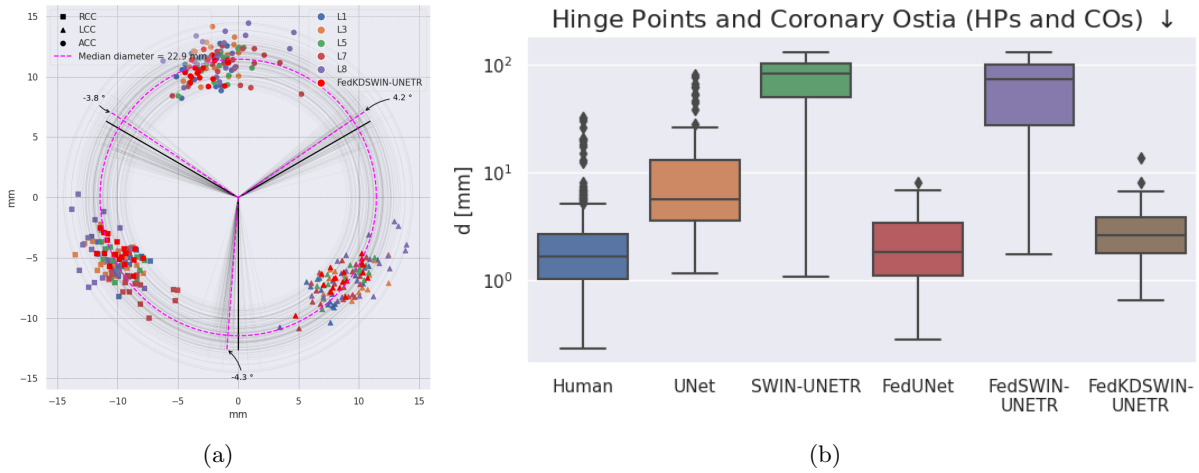


Fig. 6: Distribution of hinge point labels across annotators and boxplot of distance of annotators and trained models on public dataset ImageCAS [61], which also serves as out-of-distribution testset. a) All annotators have placed the hinge points at the correct location. However, some systematic differences can be observed (e.g. between RCC of location 2 and 4). b) Average distance from mean points. The median distance for the human annotators is around 2 mm. Convolutional networks generalize better for local (on one location only) and federated training. By using KD on a large dataset, the performance and generalizability of transformers can be significantly enhanced.

annotations is  $2.60 \pm 3.58$  mm. Using the same method for displaying the distribution of labels as in Fig. 5 the differences between human annotators from different hospitals are qualitatively explored. Despite providing a unified annotation protocol before labelling, some systematic biases can be found, e.g., between location 2 and 4 on the hinge point of the right coronary cusp (c.f. Fig. 6). For evaluation of the trained models the 2 mm pose a lower bound for the test error and our results show that our model is almost on-par (Fig. 6).

### Quantitative Evaluation on Public Dataset

Since the ImageCAS dataset [61] was not captured for TAVI patients but for inspecting the coronary arteries, a slightly different CT protocol was used. The dataset serves as an out-of-distribution validation set to verify the generalization performance of the different methods. The inter-observer variability has a mean of  $2.60 \pm 3.58$  mm, which is the lower bound the methods can reach on average. As was seen from the federated experiments the UNet based architectures can generalize better with less data samples (UNet:  $15.54 \pm 19.02$  mm, SWIN-UNETR:  $74.99 \pm 35.74$  mm). The performance of the SWIN-UNETR degrades significantly indicating overfitting. While the federated approach improves the performance of the UNet, the transformer is not improved in a meaningful way (FedUNet:  $2.47 \pm 1.69$  mm, FedSWIN-UNETR:  $74.36 \pm 33.14$  mm). However, if semi-supervised federated KD is used to pre-train the SWIN-UNETR on the large unlabeled datasets, the performance can be increased and is in range of the federated UNet approach (FedKDSWIN-UNETR:  $2.84 \pm 1.65$  mm).

### Generalizability to Downstream Task

Beyond planning of TAVI procedure, pre-procedural exclusion of relevant coronary artery disease is recommended in these patients by current guidelines [39]. To investigate the generalization performance of our trained models, we opt for segmenting the coronary arteries in the public ImageCAS dataset [61], which already includes contours of the vessel lumen for 1000 patients (80/20 train-test-split).

For segmenting the coronary arteries, we restrict ourselves to only finetune the last output layer of both models trained with KD, the UNet and SWIN-UNETR, to test the amount of meaningful features already extracted by the backbone of the federated model. In both models the last layer is a  $1 \times 1$  convolution that only reweights the feature maps from the previous layer. While the SWIN-UNETR yields a DICE score of 24.45 the UNet is only able to achieve a DICE score of 4.45. We attribute this to the learning of global context in the transformer encoder that enables better performances in foundation models compared to convolutional based ones.

## 3 Discussion

We performed the largest federated learning cardiac imaging study to date on 8124 CT scans across eight hospitals in Germany. We are the first to solve the problem of federated learning on partially labeled clients in the realm of real world medical data instead of carefully curated public challenge datasets. In addition to training on labeled subsets of the data we also leverage the unlabeled images to increase the performance with semi-supervised federated knowledge distillation from a UNet teacher model to a transformer student model (SWIN-UNETR) [12]. The predictions of the federated trained submodels are better on the other locations compared to the single models trained on each location independently. Surprisingly, the federated model often performs better than the own local trained one. We attribute this to the better generalization ability of the federated model since our annotated training subsets are sometimes quite small and exhibit inter-observer variability. The federated workflow is especially beneficial for these locations that do not possess large quantities of (labeled) data. Our distilled SWIN-UNETR can serve as a foundation model for future work on cardiac CT imaging. Moreover, we have shown its generalizability for out of distribution samples on a publicly available dataset (see Fig. 6).

The advantage of using a transformer-based model is only evident when the dataset sizes are large enough and federated training might be one ingredient to have access to many distributed data sets. However, in a setting without the presence of many human annotated samples, training transformer architectures to reach very good performance is still extremely challenging. Our two stage approach using semi-supervised knowledge distillation with a UNet teacher model seems to be one solution to this problem. When training on downstream tasks the features extracted from the SWIN-UNETR seem to be more meaningful as it performs better when only finetuning the last layer, a  $1 \times 1$  convolution posing a reweighting of the previous layer.

Compared to other federated learning studies our work is of higher complexity [36,9,24] due to different field of views and anisotropic spacing. Contrary to past studies where all labels for all tasks existed at all clients we deal with partially labeled clients that have a skewed distribution of present labels. Approaches to learning from partially labeled datasets in a federated environment include learning one encoder per participating client and label [60]. However, this is only possible if each client is in possession of only one label. Further, marginal loss [46] is a popular method for dealing with partially labeled clients [26,57]. The homogeneous distribution of anatomical structures in the human body can also be utilized in the training process to make assumptions about missing labels [62]. But the works are performed on large, relatively easy to segment structures (e.g. large organs such as liver). Different classification heads for each dataset in the training distribution also represent one way of dealing with partially labeled datasets [55]. However, this discards information from possibly intersecting labels across the datasets [54].

Further, we are the first to employ knowledge distillation in a federated environment on real world data CT cardiac imaging data. Our final model that is distilled from three teacher models can perform the tasks of point detection and segmentation simultaneously. The problem solved in this work requires expert physician knowledge in contrast to solving a problem that only has a binary discriminative outcome that can be read out from a electronic health record database. The research on federated knowledge distillation (KD) shows similarities, as these studies are conducted using publicly available datasets [20]. In KD, the predictive ability of a low-capacity student network is enhanced by training it to align its predictions with those of a high-capacity teacher network [14]. Typically, knowledge is distilled from a group of teacher networks in FL, each trained on data from a different client [45,31]. Other methods include distilling knowledge by matching attention maps between client models or aligning the feature maps of both models [10,59,52]. Wang et al. use marginal loss together with KD to learn a model across partially labeled clients. However, marginal loss was sufficient to learn all structures present in the federation in KD was employed to further enhance results [57]. As stated, this is only the case when trained on large labels that are relatively easy-to-segment.

Before being able to train a model successful in a federation many tedious and practical obstacles needed to be solved. We were only allowed to initialize communication from within the clinic networks. Further, we had to take additional security measures in the form of transport layer security (TLS) and username and password authentication. We thus opted for `fedbiomed` as our library to enable federated learning, as they support many security features out of the box [47]. Before even starting to gather the required data each location had to independently get an ethics agreement granted that allows training on that data. Although technically federated learning is an established paradigm for most legal departments the topic was new ground, which we have now covered with our study. We hope that the preprocessing and training scripts for this study can be used to accelerate further studies in the future.

Once each location had successfully applied for the ethics agreement, the downloading of data from the PACS and other clinical information systems could be initiated. Although the system is standardized even the intra-hospital variance of data was large so that site specific pre-processing was necessary. Each hospital had different preferences regarding the recorded field of view and spacing. Different naming schemes made it difficult to extract the right series for each patient. Despite all the obstacles we believe one reason why our distilled model pretrained on the unlabeled data performs better is the large data heterogeneity induced by above factors.

In addition to homogenizing data formats also the hardware and software used needed to be uniform. Each location purchased the same machine to perform the learning process. However, different requirements at each location made different installation and network specifications necessary dependent on the individual site. As unified software solution we opted for an adapted version of Kaapana [44]. It allows for flexible deployment of containerized applications. After pseudonymization or anonymization dependent on the requirements at the individual locations the data was uploaded in the integrated PACS of our platform. From there it could be exported, filtered and made available for federated training in a consistent manner across all locations. Setting up the software and hardware stack required numerous conference calls [53].

Federated learning has a privacy by design structure since no data leaves the individual hospitals. However, some works have proven that in a dishonest environment clients can either corrupt the training process or reconstruct part of model’s training data from the weights [56]. Multiple advanced privacy options exist that mitigate above points but come at the expense of model’s predictive performance. Examples include differential privacy [50,1], secure multi-party computation, and homomorphic encryption [18]. However, we assume an honest environment where we must not be concerned about individual clients wanting to corrupt the training or inference procedure.

The model weights of the federated trained SWIN-UNETR foundation model are made available as a contribution to open science to enable further research in the cardiac CT heart imaging on more and

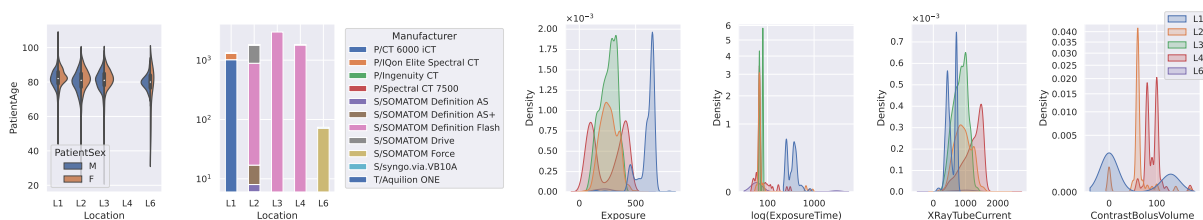


Fig. 7: Demographics of patients and data properties across clients. Some data was not available at all clients. Three manufacturers with in total eleven different models were included in the federated training. The acquisition protocols in terms of exposure, exposure time, X-ray tube current, and contrast bolus volume vary across clients. Manufacture acronyms are P: Philips, S: Siemens, T: Toshiba.

diverse downstream tasks. The federated infrastructure is planned to be re-used for more use cases within the DZHK to enable large-scale AI in cardiovascular research. Concurrently, more hospitals are joining the federated network.

## 4 Methods

This manuscript’s study and results adhere to all pertinent ethical guidelines and uphold ethical standards in both research conduct and manuscript preparation, in accordance with all relevant laws and regulations concerning human subject treatment. Each collaborating site’s private retrospective data analysis has received approval from its respective institutional review board. Each institutional review board allowed for retrospective data analysis without obtained patient consent since no data is disclosed to any participant in the federation.

### Data

This study’s data comprises patients who underwent a minimally invasive procedure for replacing their aortic valve with a Transcatheter Aortic Valve Implantation (TAVI) prosthesis. Consistent with clinical guidelines, every patient undergoes a contrast-enhanced CT scan triggered by an electrocardiogram, conducted in either only the systolic or both the systolic and diastolic phases of the heart cycle. For this study we included all available contrast enhanced CT scans not dependent whether they only had the systolic or diastolic phase available. Collective information about the demographics of the included population and CT imaging parameters is presented in Fig. 7.

The data acquisition occurred at each participating site from 2015 to 2021. Each site’s institutional review board approved the retrospective analysis of CT scans from patients who received a TAVI prosthesis during this time. However, challenges in exporting data from the PACS varied by location, preventing the complete dataset from being utilized for model training or testing at some sites. These challenges primarily involved limitations in automatically exporting large volumes of data from the internal PACS systems. Our study highlighted deficiencies in data export protocols at some institutions, which we hope will trigger investments into better data pipelines. Future studies leveraging this infrastructure can benefit from the insights we have gained.

### Harmonized Data Preprocessing

Subsequent to downloading data in the Digital Imaging and Communications in Medicine (DICOM) file format from the PACS the data was pseudonymized or anonymized dependent on the requirements from

the individual institutional review board. After successful de-identification the data was uploaded in the PACS that is included in the platform. The platform’s filtering and viewing features were utilized to gather the series descriptions of the wanted volumes. It is worth noting that there is a significant intra-hospital variance in these descriptions, indicating that they are far from being standardized. After successful identification we converted DICOMs into the Neuroimaging Informatics Technology Initiative (NIfTI) file format. This format has the advantage of removing all patient identifying information automatically from the header portion of the DICOM data. Before performing model training the region containing the heart was focused utilizing the Totalsegmentator tool [58]. Each image was normalized using a CT normalization scheme:

$$\mathbf{x}_{\text{norm}} = \frac{\text{clip}(\mathbf{X}, \mathcal{D}_{0.05}, \mathcal{D}_{0.95}) - \mu}{\max(\sigma, 1e - 8)} \quad \text{with} \quad \mu = \mathbb{E}[\mathcal{D}] \text{ and } \sigma = \sqrt{\mathbb{V}[\mathcal{D}]}, \quad (1)$$

with mean ( $\mu = -438.61$ ) standard deviation ( $\sigma = 520.98$ ) and the two percentiles ( $0.05 = -1024$  &  $0.95 = 696$ ) were taken from the TotalSegmentator pipeline [58].

Where not already present, the annotations (3D points for hinge points, origins of coronary arteries, and membranous septum, and segmentations for calcification) were obtained with the medical Medical Interaction Toolkit (MITK)<sup>3</sup>. Annotation protocols were provided in text and video form, which was reported to be very beneficial for uniform label generation.

## The Neural Network Architectures

For the three subtasks we used the popular 3D UNet with residual connections (3D-ResUNet) with 32 base filters [8,13,15]. The learning rate was set to  $lr = 0.01$  and optimized with the AdamW optimizer [27]. As loss function during training we used a combination of cross entropy and DICE score loss with deep supervision [48]. When applying deep supervision also for the intermediate outputs of the skip connections the loss function is applied to a downsampled version of the target, which has been shown to improve segmentation performance [15].

For the final model that combines the knowledge from the three subnetworks we use the new Swin UNet Transformer (Swin UNETR) [12]. We use a feature size of 24 with a patch size of  $\mathbb{R}^{96 \times 96 \times 96}$ . The learning rate was set to  $lr = 10^{-4}$  and optimized with the AdamW optimizer [27]. We equipped the transformer with three heads, one for each task, to train all tasks concurrently.

## The Federation

In federated learning multiple data holding clients train a model locally on their data shards and report the trained model weights back to a central server where averaging is performed [30,19]. After successful averaging another round of training is initiated until the model converges. Each round is termed a federated round. This allows data privacy compliant model training as no patient data ever leaves the individual hospitals boundaries. The most widespread architecture is a hub-and-spoke system where all clients train in parallel instead of an e.g. sequential training [18,36].

Our federation spans eight cardiology and radiology department in university hospitals in Germany (c.f. Fig. 1). Connection could be established only from within the individual clinics to a server that resided behind a firewall at Heidelberg University. Each model was trained for 20 federated rounds of averaging with 10 local epochs in each round. We chose to perform model weight’s aggregation using a popular variant of the federated averaging algorithm [23]. Every communication in our federation was based on transport layer security, additional authentication with username and password, and server-side

<sup>3</sup> [https://www.mitk.org/wiki/The\\_Medical\\_Imaging\\_Interaction\\_Toolkit\\_\(MITK\)](https://www.mitk.org/wiki/The_Medical_Imaging_Interaction_Toolkit_(MITK))

IP address white listing. These measures help mitigate some of the privacy and security concerns still inherent to FL.

Our work covers the whole process of extracting real world data from clinical information systems and subsequent homogenization of data formats across the different sites and label types. The federated learning software stack was installed at each location that is intended to be used beyond this study for future research. We created a custom fork of the renowned Kaapana platform [44]. It allows for a flexible deployment of containerized applications in combination to a picture archiving and communication system (PACS). To extract the cohorts needed per location we use a custom developed filtering tool described here [53]. Each data type is stored in a custom structured report template such that they can be linked to the corresponding series [53]. Segmentation objects can also be stored and linked to the referenced image series within the PACS. Fedbiomed is used as FL library as they provide very sophisticated security measures [47]. All communication is encrypted with transport layer security (TLS) encryption, where the key is distributed to the clients prior to training. Further, each client must authenticate with custom credentials (username and password). And last, IP white listing is performed such that only predefined IP addresses can initiate a connection. The connection is unidirectional. It must be initiated from within the clinic network, the clients then poll for updates such that no action can be triggered from the server without the client noticing.

## Data Availability

All data from the eight sites used in this study are not made publicly available due to restrictions imposed by the participating sites. The data was also not publicly available during conducting of this study. As by privacy-by-design definition of federated learning they were instead used locally during training and validation of the trained models. The data to reproduce the plots as well as the corresponding scripts are made publicly available under: <https://github.com/Cardio-AI/fed-foundation-model-cardiac-ct>. The ImageCAS dataset is available under: <https://github.com/XiaoweiXu/ImageCAS-A-Large-Scale-Dataset-and-Benchmark-for-Coronary-Artery-Segmentation-based-on-CT>. The corresponding labels for quantifying the inter-observer variability are available at: <https://github.com/Cardio-AI/fed-foundation-model-cardiac-ct>. The pointsets can be opened with the Medical Interaction Toolkit (MITK) available under: [https://www.mitk.org/wiki/The\\_Medical\\_Imaging\\_Interaction\\_Toolkit\\_\(MITK\)](https://www.mitk.org/wiki/The_Medical_Imaging_Interaction_Toolkit_(MITK)).

## Code Availability

Following the FAIR criteria (findability, accessibility, interoperability, and reusability) in scientific research all code used in this study is made publicly available. We used a custom fork of Kaapana [44] from <https://github.com/kaapana/kaapana> which is available under <https://github.com/Cardio-AI/kaapana> for orchestration of docker containers at each location. The federated learning library fedbiomed is available under <https://github.com/fedbiomed/fedbiomed> our custom fork with more security features enabled is available under <https://github.com/Cardio-AI/fedbiomed>. For creation of labels we use MITK [https://www.mitk.org/wiki/The\\_Medical\\_Imaging\\_Interaction\\_Toolkit\\_\(MITK\)](https://www.mitk.org/wiki/The_Medical_Imaging_Interaction_Toolkit_(MITK)). The nnUNet pipeline used for training the per-task models is available under <https://github.com/MIC-DKFZ/nnUNet>. Our preprocessing, training, and validation scripts are made available under <https://github.com/Cardio-AI/fed-foundation-model-cardiac-ct>. The pipelines were developed using PyTorch [34], MONAI [7], TorchIO [37], and SimpleITK [4].

## Acknowledgements

The project was funded by the DZHK, the Klaus Tschira Foundation within the Informatics for Life framework, and the BMBF-SWAG Project 01KD2215D.

## Author Contributions

Malte Tölle developed the presented method, conducted the experiments and evaluations, set up the federated learning software stack, and wrote the manuscript. Sandy Engelhardt organised the consortium, and significantly helped to shape the methods and the manuscript. Sebastian Eble, Moritz Bednorz, and Halvar Kelm contributed code for model training and software setup. Philipp Garthe, Lars Kaderali, Nina Krüger, Andreas Leha, Simon Martin, Clemens Scheree, Jan Moritz Seliger, and Stefan Simm were the direct contact persons at each participating location, set up the local infrastructures, and exported, curated, and uploaded the required data. Florian Andre, Peter Bannas, Norbert Frey, Stefan Groß, Alexander Meyer, Eike Nagel, Stefan Orwat, Tim Friede, Tim Seidler, and Sandy Engelhardt developed the idea for the study, provided guidance, and helped with revising the final manuscript.

## Competing interests

Norbert Frey reports speaker honoraria, presentations or advisory board consultations from AstraZeneca, Bayer AG, Boehringer Ingelheim, Novartis, Pfizer, Daiichi Sankyo Deutschland. Tim Seidler reports research, educational, or travel grants and honoraria for lectures or advisory board consultations from Abbott Vascular, AstraZeneca, Boehringer Ingelheim, Bristol Myers Squibb, Corvia, Cytokinetics, Edwards Life Sciences, Medtronic, Myocardia, Novartis, Pfizer, Teleflex. Alexander Meyer reports consulting or lecturing fees from Medtronic, Bayer, Pfizer. Clemens Scherer reports speaker honorarium from AstraZeneca. Sandy Engelhardt reports speaker honorarium from Boehringer Ingelheim. None are related to the content of the manuscript. The other authors declare no conflicts of interest.

## References

1. Abadi, M., Chu, A., Goodfellow, I., McMahan, H.B., Mironov, I., Talwar, K., Zhang, L.: Deep learning with differential privacy. In: Proceedings of the 2016 ACM SIGSAC Conference on Computer and Communications Security. p. 308–318 (2016). <https://doi.org/10.1145/2976749.2978318>
2. Aoyama, G., Zhao, L., Zhao, S., Xue, X., Zhong, Y., Yamauchi, H., Tsukihara, H., Maeda, E., Ino, K., Tomii, N., Takagi, S., Sakuma, I., Ono, M., Sakaguchi, T.: Automatic aortic valve cusps segmentation from ct images based on the cascading multiple deep neural networks. *Journal of Imaging* **8**(1) (2022). <https://doi.org/10.3390/jimaging8010011>
3. Astudillo, P., Mortier, P., Bosmans, J., De Backer, O., de Jaegere, P., De Beule, M., Dambre, J.: Enabling automated device size selection for transcatheter aortic valve implantation. *Journal of Interventional Cardiology* **2019**, 3591314 (2019). <https://doi.org/10.1155/2019/3591314>
4. Beare, R., Lowekamp, B., Yaniv, Z.: Image segmentation, registration and characterization in r with simpleitk. *Journal of Statistical Software* **86**(8), 1–35 (2018). <https://doi.org/10.18637/jss.v086.i08>
5. Bernard, O., Lalonde, A., Zotti, C., Cervenansky, F., Yang, X., Heng, P.A., Cetin, I., Lekadir, K., Camara, O., Gonzalez Ballester, M.A., Sanroma, G., Napel, S., Petersen, S., Tziritas, G., Grinias, E., Khened, M., Kollerathu, V.A., Krishnamurthi, G., Rohé, M.M., Pennec, X., Sermesant, M., Isensee, F., Jäger, P., Maier-Hein, K.H., Full, P.M., Wolf, I., Engelhardt, S., Baumgartner, C.F., Koch, L.M., Wolterink, J.M., Išgum, I., Jang, Y., Hong, Y., Patravali, J., Jain, S., Humbert, O., Jodoin, P.M.: Deep learning techniques for automatic mri cardiac multi-structures segmentation and diagnosis: Is the problem solved? *IEEE Transactions on Medical Imaging* **37**(11), 2514–2525 (2018). <https://doi.org/10.1109/TMI.2018.2837502>



6. Campello, V.M., Gkontra, P., Izquierdo, C., Martín-Isla, C., Sojoudi, A., Full, P.M., Maier-Hein, K., Zhang, Y., He, Z., Ma, J., Parreño, M., Albiol, A., Kong, F., Shadden, S.C., Acero, J.C., Sundaresan, V., Saber, M., Elattar, M., Li, H., Menze, B., Khader, F., Haarbuerger, C., Scannell, C.M., Veta, M., Carscadden, A., Punithakumar, K., Liu, X., Tsafaris, S.A., Huang, X., Yang, X., Li, L., Zhuang, X., Viladés, D., Descalzo, M.L., Guala, A., Mura, L.L., Friedrich, M.G., Garg, R., Lebel, J., Henriques, F., Karakas, M., Çavuş, E., Petersen, S.E., Escalera, S., Seguí, S., Rodríguez-Palomares, J.F., Lekadir, K.: Multi-centre, multi-vendor and multi-disease cardiac segmentation: The m&ms challenge. *IEEE Transactions on Medical Imaging* **40**(12), 3543–3554 (2021). <https://doi.org/10.1109/TMI.2021.3090082>
7. Cardoso, M.J., Li, W., Brown, R., Ma, N., Kerfoot, E., Wang, Y., Murrey, B., Myronenko, A., Zhao, C., Yang, D., Nath, V., He, Y., Xu, Z., Hatamizadeh, A., Myronenko, A., Zhu, W., Liu, Y., Zheng, M., Tang, Y., Yang, I., Zephyr, M., Hashemian, B., Alle, S., Darestani, M.Z., Budd, C., Modat, M., Vercauteren, T., Wang, G., Li, Y., Hu, Y., Fu, Y., Gorman, B., Johnson, H., Genereaux, B., Erdal, B.S., Gupta, V., Diaz-Pinto, A., Dourson, A., Maier-Hein, L., Jaeger, P.F., Baumgartner, M., Kalpathy-Cramer, J., Flores, M., Kirby, J., Cooper, L.A.D., Roth, H.R., Xu, D., Bericat, D., Floca, R., Zhou, S.K., Shuaib, H., Farahani, K., Maier-Hein, K.H., Aylward, S., Dogra, P., Ourselin, S., Feng, A.: Monai: An open-source framework for deep learning in healthcare (2022). <https://doi.org/10.48550/arXiv.2211.02701>
8. Çiçek, Ö., Abdulkadir, A., Lienkamp, S., Brox, T., Ronneberger, O.: 3d u-net: Learning dense volumetric segmentation from sparse annotation. In: *Medical Image Computing and Computer-Assisted Intervention (MICCAI)*. vol. 9901, pp. 424–432 (2016)
9. Dayan, I., Roth, H.R., Zhong, A., Harouni, A., Gentili, A., Abidin, A.Z., Liu, A., Costa, A.B., Wood, B.J., Tsai, C.S., et al.: Federated learning for predicting clinical outcomes in patients with covid-19. *Nature Medicine* **27**(10), 1735–1743 (2021). <https://doi.org/10.1038/s41591-021-01506-3>
10. Gong, X., Sharma, A., Karanam, S., Wu, Z., Chen, T., Doermann, D., Innanje, D.: Ensemble attention distillation for privacy-preserving federated learning. In: *International Conference on Computer Vision* (2021). <https://doi.org/10.1109/ICCV48922.2021.01480>
11. Génereux, P., Head, S.J., Wood, D.A., Kodali, S.K., Williams, M.R., Paradis, J.M., Spaziano, M., Kappetein, A.P., Webb, J.G., Cribier, A., Leon, M.B.: Transcatheter aortic valve implantation 10-year anniversary: review of current evidence and clinical implications. *European Heart Journal* **33**(19), 2388–2398 (2012). <https://doi.org/10.1093/eurheartj/ehs220>
12. Hatamizadeh, A., Nath, V., Tang, Y., Yang, D., Roth, H.R., Xu, D.: Swin unetr: Swin transformers for semantic segmentation of brain tumors in mri images. In: *Brainlesion: Glioma, Multiple Sclerosis, Stroke and Traumatic Brain Injuries*. pp. 272–284 (2022). [https://doi.org/10.1007/978-3-031-08999-2\\_22](https://doi.org/10.1007/978-3-031-08999-2_22)
13. He, K., Zhang, X., Ren, S., Sun, J.: Deep residual learning for image recognition. In: *2016 IEEE Conference on Computer Vision and Pattern Recognition (CVPR)*. pp. 770–778 (2016). <https://doi.org/10.1109/CVPR.2016.90>
14. Hinton, G., Vinyals, O., Dean, J.: Distilling the knowledge in a neural network. In: *Advances in Neural Information Processing Systems Workshop* (2014). <https://doi.org/arXiv:1503.02531>
15. Isensee, F., Jaeger, P.F., Kohl, S.A.A., Petersen, J., Maier-Hein, K.H.: nnu-net: a self-configuring method for deep learning-based biomedical image segmentation. *Nature Methods* **18**(2), 203–211 (2021). <https://doi.org/10.1038/s41592-020-01008-z>
16. Jørgensen, T.H., Hansson, N., De Backer, O., Bieliauskas, G., Terkelsen, C.J., Wang, X., Jensen, J.M., Christiansen, E.H., Piazza, N., Svendsen, J.H., et al.: Membranous septum morphology and risk of conduction abnormalities after transcatheter aortic valve implantation. *EuroIntervention* **17**(13), 1061–1069 (2022). <https://doi.org/10.4244/EIJ-D-21-00363>
17. Kaissis, G., Ziller, A., Passerat-Palmbach, J., Ryffel, T., Usynin, D., Trask, A., Lima, I., Mancuso, J., Jungmann, F., Steinborn, M.M., et al.: End-to-end privacy preserving deep learning on multi-institutional medical imaging. *Nature Machine Intelligence* **3**(6), 473–484 (2021). <https://doi.org/10.1038/s42256-021-00337-8>
18. Kaissis, G.A., Makowski, M.R., Rückert, D., Braren, R.F.: Secure, privacy-preserving and federated machine learning in medical imaging. *Nature Machine Intelligence* **2**(6), 305–311 (2020). <https://doi.org/10.1038/s42256-020-0186-1>
19. Karimireddy, S.P., Kale, S., Mohri, M., Reddi, S., Stich, S., Suresh, A.T.: SCAFFOLD: Stochastic controlled averaging for federated learning. In: *Proceedings of the 37th International Conference on Machine Learning. Proceedings of Machine Learning Research*, vol. 119, pp. 5132–5143 (2020)

20. Kim, S., Park, H., Kang, M., Jin, K.H., Adeli, E., Pohl, K.M., Park, S.H.: Federated learning with knowledge distillation for multi-organ segmentation with partially labeled datasets. *Medical Image Analysis* **95**, 103156 (2024). <https://doi.org/10.1016/j.media.2024.103156>
21. Krüger, N., Meyer, A., Tautz, L., Hüllebrand, M., Wamala, I., Pullig, M., Kofler, M., Kempfert, J., Sündermann, S., Falk, V., Hennemuth, A.: Cascaded neural network-based ct image processing for aortic root analysis. *International Journal of Computer Assisted Radiology and Surgery* **17**(3), 507–519 (2022). <https://doi.org/10.1007/s11548-021-02554-3>
22. Leon, M.B., Smith, C.R., Mack, M., Miller, D.C., Moses, J.W., Svensson, L.G., Tuzcu, E.M., Webb, J.G., Fontana, G.P., Makkar, R.R., et al.: Transcatheter aortic-valve implantation for aortic stenosis in patients who cannot undergo surgery. *The New England Journal of Medicine* **363**(17), 1597–1607 (2010). <https://doi.org/10.1056/NEJMoa1008232>
23. Li, T., Sahu, A.K., Zaheer, M., Sanjabi, M., Talwalkar, A., Smith, V.: Federated optimization in heterogeneous networks. In: *MLSys* (2020). <https://doi.org/10.48550/arXiv.1812.06127>
24. Linardos, A., Kushibar, K., Walsh, S., Gkontra, P., Lekadir, K.: Federated learning for multi-center imaging diagnostics: a simulation study in cardiovascular disease. *Nature Scientific Reports* **12**(1), 3551 (2022). <https://doi.org/10.1038/s41598-022-07186-4>
25. Liu, J., Zhang, Y., Chen, J.N., Xiao, J., Lu, Y., Landman, B.A., Yuan, Y., Yuille, A., Tang, Y., Zhou, Z.: Clip-driven universal model for organ segmentation and tumor detection (2023). <https://doi.org/10.1109/ICCV51070.2023.01934>
26. Liu, P., Sun, M., Zhou, S.K.: Multi-site organ segmentation with federated partial supervision and site adaptation (2023)
27. Loshchilov, I., Hutter, F.: Decoupled weight decay regularization. In: *International Conference on Learning Representations* (2019). <https://doi.org/arxiv:1711.05101>
28. Mauri, V., Frohn, T., Deuschl, F., Mohamed, K., Kuhr, K., Reimann, A., Körber, M.I., Schofer, N., Adam, M., Friedrichs, K., Kuhn, E.W., Scholtz, S., Rudolph, V., Wahlers, T.C.W., Baldus, S., Mader, N., Schäfer, U., Rudolph, T.K.: Impact of device landing zone calcification patterns on paravalvular regurgitation after transcatheter aortic valve replacement with different next-generation devices. *Open Heart* **7**(1) (2020). <https://doi.org/10.1136/openhrt-2019-001164>
29. Maurício, J., Domingues, I., Bernardino, J.: Comparing vision transformers and convolutional neural networks for image classification: A literature review. *Applied Sciences* **13**(9) (2023). <https://doi.org/10.3390/app13095521>
30. McMahan, H.B., Moore, E., Ramage, D., Hampson, S., y Arcas, B.A.: Communication-efficient learning of deep networks from decentralized data. In: *AISTATS* (2017)
31. Mora, A., Tenison, I., Bellavista, P., Rish, I.: Knowledge distillation for federated learning: a practical guide (2022). <https://doi.org/arXiv:2211.04742>
32. Musallam, A., Buchanan, K., Yerasi, C., Dheendsa, A., Zhang, C., Shea, C., Case, B., Forrestal, B., Satler, L., Ben-Dor, I., Torguson, R., Rogers, T., Waksman, R.: Impact of left ventricular outflow tract calcification on outcomes following transcatheter aortic valve replacement. *Cardiovascular Revascularization Medicine* **35**, 1–7 (2022). <https://doi.org/10.1016/j.carrev.2021.07.010>
33. Oquab, M., Darcet, T., Moutakanni, T., Vo, H.V., Szafraniec, M., Khalidov, V., Fernandez, P., Haziza, D., Massa, F., El-Nouby, A., Howes, R., Huang, P.Y., Xu, H., Sharma, V., Li, S.W., Galuba, W., Rabbat, M., Assran, M., Ballas, N., Synnaeve, G., Misra, I., Jegou, H., Mairal, J., Labatut, P., Joulin, A., Bojanowski, P.: Dinov2: Learning robust visual features without supervision (2023). <https://doi.org/arXiv:2304.07193>
34. Paszke, A., Gross, S., Massa, F., Lerer, A., Bradbury, J., Chanan, G., Killeen, T., Lin, Z., Gimelshein, N., Antiga, L., Desmaison, A., Kopf, A., Yang, E., DeVito, Z., Raison, M., Tejani, A., Chilamkurthy, S., Steiner, B., Fang, L., Bai, J., Chintala, S.: Pytorch: An imperative style, high-performance deep learning library. In: *Advances in Neural Information Processing Systems*. vol. 32 (2019). <https://doi.org/10.5555/3454287.3455008>
35. Pati, S., Baid, U., Edwards, B., Sheller, M., Wang, S.H., Reina, G.A., Foley, P., Gruzdev, A., Karkada, D., Davatzikos, C., et al.: Federated learning enables big data for rare cancer boundary detection. *Nature Communications* **13**(1), 7346 (2022). <https://doi.org/10.1038/s41467-022-33407-5>
36. Pati, S., Baid, U., Zenk, M., Edwards, B., Sheller, M., Reina, G.A., Foley, P., Gruzdev, A., Martin, J., Albarqouni, S., Chen, Y., Shinohara, R.T., Reinke, A., Zimmerer, D., Freymann, J.B., Kirby, J.S., Davatzikos,

- C., Colen, R.R., Kotrotsou, A., Marcus, D., Milchenko, M., Nazer, A., Fathallah-Shaykh, H., Wiest, R., Jakab, A., Weber, M.A., Mahajan, A., Maier-Hein, L., Kleesiek, J., Menze, B., Maier-Hein, K., Bakas, S.: The federated tumor segmentation (fets) challenge (2021). <https://doi.org/10.5281/zenodo.10990499>
37. Pérez-García, F., Sparks, R., Ourselin, S.: Torchio: A python library for efficient loading, preprocessing, augmentation and patch-based sampling of medical images in deep learning. *Computer Methods and Programs in Biomedicine* **208**, 106236 (2021). <https://doi.org/10.1016/j.cmpb.2021.106236>
  38. Rahimi, S., Oktay, O., Alvarez-Valle, J., Bharadwaj, S.: Addressing the exorbitant cost of labeling medical images with active learning. In: *International Conference on Machine Learning and Medical Imaging and Analysis* (2021)
  39. Renker, M., Korosoglou, G.: The role of computed tomography prior to transcatheter aortic valve implantation: preprocedural planning and simultaneous coronary artery assessment. *Journal of Thoracic Disease* **16**(2), 833–838 (2024). <https://doi.org/10.21037/jtd-23-1384>
  40. Rieke, N., Hancox, J., Li, W., Milletari, F., Roth, H.R., Albarqouni, S., Bakas, S., Galtier, M.N., Landman, B.A., Maier-Hein, K., Ourselin, S., Sheller, M., Summers, R.M., Trask, A., Xu, D., Baust, M., Cardoso, M.J.: The future of digital health with federated learning **3**(119), 2398–6352 (2020). <https://doi.org/10.1038/s41746-020-00323-1>
  41. Rädtsch, T., Reinke, A., Weru, V., Tizabi, M.D., Schreck, N., Kavur, A.E., Pekdemir, B., Roß, T., Kopp-Schneider, A., Maier-Hein, L.: Labelling instructions matter in biomedical image analysis. *Nature Machine Intelligence* **5**(3), 273–283 (2023). <https://doi.org/10.1038/s42256-023-00625-5>
  42. Sadilek, A., Liu, L., Nguyen, D., Kamruzzaman, M., Serghiou, S., Rader, B., Ingerman, A., Mellem, S., Kairouz, P., Nsoesie, E.O., MacFarlane, J., Vullikanti, A., Marathe, M., Eastham, P., Brownstein, J.S., Arcas, B.A.y., Howell, M.D., Hernandez, J.: Privacy-first health research with federated learning. *npj Digital Medicine* **4**(1), 132 (2021). <https://doi.org/10.1038/s41746-021-00489-2>
  43. Sammour, Y., Krishnaswamy, A., Kumar, A., Puri, R., Tarakji, K.G., Bazarbashi, N., Harb, S., Griffin, B., Svensson, L., Wazni, O., Kapadia, S.R.: Incidence, predictors, and implications of permanent pacemaker requirement after transcatheter aortic valve replacement. *JACC: Cardiovascular Interventions* **14**(2), 115–134 (2021). <https://doi.org/10.1016/j.jcin.2020.09.063>
  44. Scherer, J., Nolden, M., Kleesiek, J., Metzger, J., Kades, K., Schneider, V., Bach, M., Sedlaczek, O., Bucher, A.M., Vogl, T.J., Grünwald, F., Kühn, J.P., Hoffmann, R.T., Kotzerke, J., Bethge, O., Schimmöller, L., Antoch, G., Müller, H.W., Daul, A., Nikolaou, K., la Fougère, C., Kunz, W.G., Ingrisich, M., Schachtner, B., Rieke, J., Bartenstein, P., Nensa, F., Radbruch, A., Umutlu, L., Forsting, M., Seifert, R., Herrmann, K., Mayer, P., Kauczor, H.U., Penzkofer, T., Hamm, B., Brenner, W., Kloeckner, R., Düber, C., Schreckenberger, M., Braren, R., Kaissis, G., Makowski, M., Eiber, M., Gafita, A., Trager, R., Weber, W.A., Neubauer, J., Reiser, M., Bock, M., Bamberg, F., Hennig, J., Meyer, P.T., Ruf, J., Haberkorn, U., Schoenberg, S.O., Kuder, T., Neher, P., Floca, R., Schlemmer, H.P., Maier-Hein, K.: Joint imaging platform for federated clinical data analytics. *JCO Clinical Cancer Informatics* **4**, 1027–1038 (2020). <https://doi.org/10.1200/CCI.20.00045>
  45. Seo, H., Park, J., Oh, S., Bennis, M., Kim, S.L.: Federated knowledge distillation. In: *Machine Learning and Wireless Communications* (2022). <https://doi.org/10.1017/9781108966559>
  46. Shia, G., Xiaoa, L., Chenb, Y., Zhoua, S.K., Zhou, K.: Marginal loss and exclusion loss for partially supervised multi-organ segmentation. *Medical image analysis* **70**, 101979 (2020). <https://doi.org/10.1016/j.media.2021.101979>
  47. Silva, S., Altmann, A., Gutman, B., Lorenzi, M.: Fed-biomed: A general open-source frontend framework for federated learning in healthcare. In: *Domain Adaptation and Representation Transfer, and Distributed and Collaborative Learning*. pp. 201–210 (2020). [https://doi.org/10.1007/978-3-030-60548-3\\_20](https://doi.org/10.1007/978-3-030-60548-3_20)
  48. Sudre, C.H., Li, W., Vercauteren, T., Ourselin, S., Jorge Cardoso, M.: Generalised Dice Overlap as a Deep Learning Loss Function for Highly Unbalanced Segmentations. *Deep learning in medical image analysis and multimodal learning for clinical decision support* pp. 240–248 (2017). [https://doi.org/10.1007/978-3-319-67558-9\\_28](https://doi.org/10.1007/978-3-319-67558-9_28)
  49. Ogier du Terrail, J., Leopold, A., Joly, C., Béguier, C., Andreux, M., Maussion, C., Schmauch, B., Tramel, E.W., Bendjebbar, E., Zaslavskiy, M., et al.: Federated learning for predicting histological response to neoadjuvant chemotherapy in triple-negative breast cancer. *Nature Medicine* **29**(1), 135–146 (2023). <https://doi.org/10.1038/s41591-022-02155-w>

50. Tölle, M., Köthe, U., André, F., Meder, B., Engelhardt, S.: Content-aware differential privacy with conditional invertible neural networks. In: Distributed, Collaborative, and Federated Learning, and Affordable AI and Healthcare for Resource Diverse Global Health. pp. 89–99 (2022). [https://doi.org/10.1007/978-3-031-18523-6\\_9](https://doi.org/10.1007/978-3-031-18523-6_9)
51. Touvron, H., Lavril, T., Izacard, G., Martinet, X., Lachaux, M.A., Lacroix, T., Rozière, B., Goyal, N., Hambro, E., Azhar, F., Rodriguez, A., Joulin, A., Grave, E., Lample, G.: Llama: Open and efficient foundation language models (2023). <https://doi.org/arXiv:2302.13971>
52. Tung, F., Mori, G.: Similarity-preserving knowledge distillation. In: Computer Vision and Pattern Recognition (2019). <https://doi.org/10.1109/ICCV.2019.00145>
53. Tölle, M., Burger, L., Kelm, H., Engelhardt, S.: Towards unified multi-modal dataset creation for deep learning utilizing structured reports. In: German Workshop on Medical Image Computing (2024)
54. Tölle, M., Navarro, F., Eble, S., Wolf, I., Menze, B., Engelhardt, S.: Funavg: Federated uncertainty weighted averaging for distributed datasets with diverse labels. In: Medical Image Computing and Computer-Assisted Intervention (MICCAI) (2024)
55. Ulrich, C., Isensee, F., Wald, T., Zenk, M., Baumgartner, M., Maier-Hein, K.H.: Multitalent: A multi-dataset approach to medical image segmentation. In: International Conference on Medical Image Computing and Computer Assisted Interventions (2023)
56. Usynin, D., Ziller, A., Makowski, M., Braren, R., Rueckert, D., Glocker, B., Kaissis, G., Passerat-Palmbach, J.: Adversarial interference and its mitigations in privacy-preserving collaborative machine learning. *Nature Machine Intelligence* (2021). <https://doi.org/10.1038/s42256-021-00390-3>
57. Wang, P., Shen, C., Wang, W., Oda, M., Fuh, C.S., Mori, K., Roth, H.R.: Condistfl: Conditional distillation for federated learning from partially annotated data. In: Celebi, M.E., Salekin, M.S., Kim, H., Albarqouni, S., Barata, C., Halpern, A., Tschandl, P., Combalia, M., Liu, Y., Zamzmi, G., Levy, J., Rangwala, H., Reinke, A., Wynn, D., Landman, B., Jeong, W.K., Shen, Y., Deng, Z., Bakas, S., Li, X., Qin, C., Rieke, N., Roth, H., Xu, D. (eds.) *Medical Image Computing and Computer Assisted Intervention – MICCAI 2023 Workshops*. pp. 311–321 (2023). [https://doi.org/10.1007/978-3-031-47401-9\\_30](https://doi.org/10.1007/978-3-031-47401-9_30)
58. Wasserthal, J., Breit, H.C., Meyer, M.T., Pradella, M., Hinck, D., Sauter, A.W., Heye, T., Boll, D., Cyriac, J., Yang, S., Bach, M., Segeroth, M.: Totalsegmentator: robust segmentation of 104 anatomical structures in ct images. *Radiology: Artificial Intelligence* **5**(5) (2023). <https://doi.org/10.1148/ryai.230024>
59. Wu, C., Wu, F., Lyu, L., Huang, Y., Lie, X.: Communication-efficient federated learning via knowledge distillation. In: *Nature Communications* (2022). <https://doi.org/10.1038/s41467-022-29763-x>
60. Xu, X., Deng, H.H., Gateno, J., Yan, P.: Federated multi-organ segmentation with inconsistent labels. *IEEE Transactions on Medical Imaging* **42**(10), 2948–2960 (2023). <https://doi.org/10.1109/TMI.2023.3270140>
61. Zeng, A., Wu, C., Lin, G., Xie, W., Hong, J., Huang, M., Zhuang, J., Bi, S., Pan, D., Ullah, N., Khan, K.N., Wang, T., Shi, Y., Li, X., Xu, X.: Imagecas: A large-scale dataset and benchmark for coronary artery segmentation based on computed tomography angiography images. *Computerized Medical Imaging and Graphics* **109**, 102287 (2023). <https://doi.org/10.1016/j.compmedimag.2023.102287>
62. Zhou, Y., Li, Z., Bai, S., Wang, C., Chen, X., Han, M., Fishman, E.K., Yuille, A.L.: Prior-aware neural network for partially-supervised multi-organ segmentation. 2019 IEEE/CVF International Conference on Computer Vision (ICCV) pp. 10671–10680 (2019). <https://doi.org/10.1109/ICCV.2019.01077>